A Comparative Study on Computation of Cumulative Distribution Function in Predicting Time of Failure of Engineering Systems

Gina Sierra[1], Matthew Daigle[2], and Kai Goebel[3]

[1]*SGT, Inc., NASA Ames Research Center, Moffett Field, CA 94035, USA*
gina.sierra@nasa.gov

[2]*NIO USA, Inc., San Jose, CA 95134*
matthew.daigle@nio.io

[3]*Palo Alto Research Center, Palo Alto, CA 94304*
kai.goebel@parc.com

ABSTRACT

Estimating accurate Time-of-Failure (ToF) of a system is key in making the decisions that impact operational safety and optimize cost. In this context, it is interesting to note that different approaches have been explored to tackle the problem of estimating ToF. The difference is in part characterized by different definitions of the hazard zones. The conventional definition for the cumulative distribution function (CDF) calculation is assumed to have well-defined hazard zones, that is, hazard zones defined as a function of the system state trajectory. An alternate method suggests the use of hazard zones defined as a function of the system state at time k, instead of hazard zones defined as a function of system state up to and including time k (Acuña and Orchard 2018, 2017). This paper explores these differences and their impact on ToF estimation. Results for the conventional CDF definition indicated that, (*i*) the cumulative distribution function is always an increasing function of time, even when realizations of the degradation process are not monotonic, (*ii*) the sum of all probabilities is always 1 and does not need to be normalized, and (*iii*) all probabilities are positive and less than or equal to 1. Similar results are not observed for CDF calculation with hazard zones defined as a function only of the system state at time k. Results for ToF estimation using Acuña's definition differ, suggesting that there is an underlying assumption of independence in the hazard zone definition. Therefore, we present an alternate definition of hazard zone which guarantees the properties of a well-defined CDF with a more straightforward ToF definition.

NOTATION

X_k	random variable that describes a system state at time k.
$x_k^{(i)}$	realization of X_k, that is, realization of the system state associated with the i^{th} trajectory at time k.
$\mathbf{X}$	vector of random variables where each random variable describes the system state at every time step, that is, the stochastic process that represents the evolution in time of the system state.
$\mathbf{x}^{(i)}$	vector of realizations of $\mathbf{X}$, that is, realization of the system state trajectory associated with the i^{th} trajectory.
$p(\cdot)$	Probability density function
$P(\cdot)$	Probability mass function
$h(\cdot)$	Hazard zone function
$I(\cdot)$	Hazard zone indicator function

1. INTRODUCTION

The benefits of estimation of Time-of-Failure (ToF) of a system include but are not limited to: undertake remedial actions to prevent the failure, extend the time until it happens, schedule maintenance at a convenient time, or prepare for the failure in a fashion that minimizes the negative effects (Goebel et al. 2017). Thus, proper characterization of the ToF is essential for decision-making processes. In this regard, different definitions for computation of the probability of failure have been explored which differ on the definition of the hazard zone function. Hazard zones are all possible system states under which the system undergoes a catastrophic failure. Hazard zone functions are functions of the system states which describe those regions in the state space that include all possible states under which the system undergoes a failure.

With the purpose of estimating the ToF of a component or system, sampling-based approaches have been widely adopted. In these approaches a population of samples is obtained from the state posterior PDF at the time when prognosis is initiated. Then, each of the samples is used as an initial condition for simulating state trajectories in "random walk" fashion iterating the state transition equation with random realizations of the process noise. At each iteration, the hazard zone function is evaluated in order to identify if the system states reached the hazard zone. This latter information is used to compute the failure distribution as a cumulative distribution function that describes the probability of failure up to and including k time.

While the ***state transition equation*** assumes the system is healthy, simulated state ***trajectories*** may migrate from a healthy region to a failure region and then migrate from the failure region to a healthy region. Due to the nature of the random process the trajectories do not exhibit strictly monotonic behavior.

With the assumption that a system can actually only fail once, hazard zone functions should identify a trajectory that reached the hazard zone at the k^{th} iteration or at previous iterations. Namely, the hazard zone function needs to be trajectory-dependent function instead of state-dependent one. However, previous works reported in the literature defines the hazard zone function as a function of only the system state at the k^{th}iteration (Orchard and Vachtsevanos 2009; Pola et al. 2015), which leads to inaccurate estimations of the ToF.

In this work we present an alternate definition of hazard zone as a function of system states up to and including time k, which guarantees that for the estimated ToF: (*i*) the cumulative distribution function is always an increasing function of time, even when realizations of the degradation process are not monotonic, (*ii*) the sum of all probabilities is always 1 and does not need to be normalized, and (*iii*) all probabilities are positive and less than or equal to 1.

This paper is organized as follows. Section 2 presents a background on the definition of probability of failure in a more general context. In Section 3, the probability of failure is defined specifically for the prognostic context. Section 4 describes other definitions of probability of failure recently reported in the literature for the prognostic context. Section 5 illustrates and discusses the impact on ToF estimation when the probability of failure is calculated with a well-defined hazard zone, that is, a hazard zone defined as a function of the system state trajectory, and calculated with an ill-defined hazard zone, that is, a hazard zone defined as a function of the system state at time k, instead of hazard zones defined as a function of system state up to and including time k. Section 6 compares the cumulative distribution function obtained through the conventional definition of probability of failure and through the Acuña's definition for dependent and independent variables. Finally, Section 7 ends with conclusions.

2. BACKGROUND

Let $\mathbf{A}$ be the input and B be the output of the model, $B = g(\mathbf{A})$, that characterizes the performance of a system. Since there are uncertainties associated with the model inputs, $\mathbf{A} = (A_1, A_2, \ldots, A_n)$ represent the input random variables with PDF $f_{A_i}(a_i)$ and joint PDF $f_{A_1,A_2,\ldots,A_n}(a_1, a_2, \ldots, a_n)$.

If a failure is defined by the event $g(\mathbf{A}) \le b$, that is, the event when the performance function, $B = g(\mathbf{A})$, reaches a certain threshold, the probability of failure is then defined as the CDF of B, $p_f = P(g(\mathbf{A}) \le b)$, and is calculated by (Prob. Engineering Design n.d.):

$$\begin{aligned} p_f &= \int \cdots \int_{g(\mathbf{a}) \le b} f_{A_1,A_2,\ldots,A_n}(a_1, a_2, \ldots, a_n) da_1 da_2 \ldots da_n \\ &= \int_{g(\mathbf{a}) \le b} f_{\mathbf{A}}(\mathbf{a}) d\mathbf{a} \end{aligned} \tag{1}$$

If all the random variables are independent,

$$p_f = \int \cdots \int_{g(\mathbf{a}) \le b} \prod_{i=1}^{n} f_{A_i}(a_i) da_1 da_2 \ldots da_n \tag{2}$$

There are a number of complexities in the evaluation of the integration in Eq. (1): (*i*) The function $g(\mathbf{A})$ is usually a nonlinear function of $\mathbf{A}$; therefore, the integration boundary is nonlinear; (*ii*) Multidimensional integration is involved; (*iii*) In many cases the evaluation of $g(\mathbf{a})$ is computationally expensive. Hence, there is rarely a closed-form solution to the probability integration, and it is also often difficult to evaluate the probability with numerical methods. Therefore, numerical approximation methods, such as the sampling-based approaches, have been adopted to solve the probability integration (Prob. Engineering Design n.d.).

3. COMPUTING THE PROBABILITY OF FAILURE IN THE PROGNOSTIC CONTEXT

Prognosis schemes can be understood as the result of long-term predictions describing the evolution of a fault indicator, with the purpose of estimating the *Time-of-Failure* (ToF) of a component or system, from the initial conditions of the fault indicator given by the estimation stage.

The prediction of critical events requires the existence of at least one critical system state that provides the severity of the studied condition. It is always possible to combine different system states to obtain one unique fault indicator. Then, it is possible to describe the evolution in time of the dimension of the fault through non-linear state equations of the system model.

Consider $\{X_k, k \in \mathbb{N}\}$ as a Markov process denoting a state-space representation of the dynamic nonlinear system:

$$\begin{aligned} x_k &= f(x_{k-1}, w_{k-1}) \\ y_k &= g(x_k, v_k), \end{aligned} \tag{3}$$

where x_k denotes an n_x-dimensional system state vector with initial distribution $p(x_0)$ and transition probability $p(x_k|x_{k-1})$, y_k denotes the n_y-dimensional conditionally-independent noisy observations, and w_k and v_k denote independent random variables.

For the generation of long-term predictions, consider the τ-step prediction for the fault indicator (one state system of a combination of different system states) PDF $\hat{p}(x_{k_p+\tau}|y_{1:k_p})$ which describes the state distribution at the future instant $k_p + \tau$, ($\tau = 1, \ldots, m$). With the assumption that the current particle population $\left\{x_{k_p}^{(i)}, w_{k_p}^{(i)}\right\}_{i=1,\ldots,N}$ is a good representation of the system state PDF at time k_p, then it is possible to approximate the predicted fault indicator PDF at time $k = k_p + \tau$, by sequentially applying the Chapman-Kolmogorov equation, as shown in Eq. (4), and then updating each particle by sampling from the transition kernel.

$$\begin{aligned} p(x_k|y_{1:k_p}) &\approx \hat{p}(x_k|y_{1:k_p}) \\ &= \sum_{i=1}^{N} p(x_k|x_{k-1}^{(i)})\hat{p}(x_{k-1}^{(i)}|y_{1:k_p}) \\ &\approx \sum_{i=1}^{N} w_k^{(i)} \delta_{x_k^{(i)}}(x_k). \end{aligned} \tag{4}$$

In other words, a population of samples is obtained from the state posterior PDF at the beginning of prognosis. Then, each of them is used as an initial condition for simulating state trajectories in "random walk" fashion iterating the state transition equation with random realizations of the process noise. Note that the random variables in the context of prognostic are dependent.

Considering k_p as the time at which prognostics are executed, and assuming that one of the states corresponds to the fault indicator, let $\mathbf{X} = (X_{k_p}, X_{k_p+1}, \ldots, X_{k-1}, X_k)$ be the collection of random variables (the stochastic process) that represents the evolution in time of the system state associated with the fault indicator, $\mathbf{x} = (x_{k_p}, x_{k_p+1}, \ldots, x_{k-1}, x_k)$ be realizations of the stochastic process that represents the evolution of the fault indicator, and $f_{X_{k_p}, X_{k_p+1}, \ldots, X_k}$ be the joint PDF of $\mathbf{X}$. Note that X_{k_p} is the estimated fault indicator at k_p given the set of measurements $y_{1:k_p}$.

Also, let failure be defined by the event $h(\mathbf{X}) \leq y$, that is, the event when the performance function, $Y = h(\mathbf{X})$, reaches a certain threshold, y. With the occurrence of this event, the state of the system will change from safety to failure. For example, if the threshold is defined to be zero, then $Y = h(\mathbf{x}) = 0$ divides the random variable space into two well-differentiated regions: safe regions and failure regions (or *hazard zones*). When $h(\mathbf{x}) \leq 0$, the system can no longer fulfill the function for which it was designed, that is, the system undergoes a catastrophic failure (Prob. Engineering Design n.d.). Note that $h(\mathbf{x})$ is a function of the fault indicator trajectory (or system state trajectory), not a function of the fault indicator at specific time k.

The stochastic state-space representation of the system is used to compute the failure distribution as a cumulative distribution function that describes the probability of failure up to and including time k:

$$\begin{aligned} \mathcal{P}(ToF \leq k) &= \int \cdots \int_{h(\mathbf{x}) \leq y} f_{X_{k_p}, X_{k_p+1}, \ldots, X_k}(x_{k_p}, x_{k_p+1}, \ldots, x_k) dx_{k_p} dx_{k_p+1} \ldots dx_k \\ &= \int_{h(\mathbf{x}) \leq y} f_{\mathbf{X}}(\mathbf{x}) d\mathbf{x} \end{aligned} \tag{5}$$

Given the aforementioned definition of the hazard zone, and specifically the simplest hazard zone, namely a time-invariant and deterministic hazard zone, Eq. (5) can be rewritten as:

$$\mathcal{P}(ToF \leq k) = \int_{-\infty}^{\infty} I(\mathbf{x}) f_X(\mathbf{x}) d\mathbf{x} \tag{6}$$

where $I(\cdot)$ is an indicator function, which is defined by:

$$I(\mathbf{x}) = \begin{cases} 1, & h(\mathbf{x}) \leq y; \\ 0, & \text{otherwise.} \end{cases} \tag{7}$$

Remember that the *mean value* of a random variab*le* is defined as the first moment measured about the origin,

$$\mu_X = \int_{-\infty}^{\infty} x f_X(x) dx \tag{8}$$

If there are *n* samples of the random variable X, $(x_1, x_2, \ldots, x_n)$, the average of the samples is calculated by

$$\bar{X} = \sum_{i=1}^{n} x_i \cdot p(x_i) \tag{9}$$

Hence, the integral on the right-hand side of the Eq. (6) is simply the expected value of $I(\mathbf{x})$.

$$\begin{aligned}\mathcal{P}(ToF \leq k) &= \sum_{i=1}^{N} I(\mathbf{x}^{(i)}) \cdot w^{(i)} \\ &= \sum_{i=1}^{N} I(x_{k_p}^{(i)}, \ldots, x_{k-1}^{(i)}, x_k^{(i)}) \cdot w^{(i)}\end{aligned} \tag{10}$$

In the Monte Carlo sampling case, Eq. (10) can simply be estimated by:

$$\mathcal{P}(ToF \leq k) = \bar{I}(\mathbf{x}) = \frac{1}{N}\sum_{i=1}^{N} I(\mathbf{x}^{(i)}) = \frac{N_f}{N} \tag{11}$$

where N_f is the number of predicted fault indicator ***trajectories*** (not the fault indicator or system state at time k) that have the performance function less than or equal to zero, i.e. $h(\mathbf{x}) \leq 0$.

It should be noted that $I(\mathbf{x})$ is a function of the trajectory of the fault indicator from k_p to k, and its range is defined in the interval $[0,1]$. Namely, $I(\mathbf{x}): \mathbb{R}^{n_\mathbf{x}} \to [0,1]$.

In addition, $I(\mathbf{x})$ should be defined in such a way that the following hold:

1. $0 \leq \mathcal{P}(ToF \leq k) \leq 1, \forall k \in \mathbb{N}$
2. $\lim_{k\to\infty} \mathcal{P}(ToF \leq k) = 1$.

4. OTHER APPROACHES FOR THE COMPUTATION OF THE PROBABILITY OF FAILURE IN THE CONTEXT OF PROGNOSTICS

The authors in (Orchard and Vachtsevanos 2009; Pola et al. 2015) define the probability of failure at any time instant k by the expression,

$$P(ToF \leq k) = \sum_{i=1}^{N_p} w_k^{(i)} \mathcal{P}(failure | X = x_k^{(i)}) \tag{12}$$

where $p(failure|X)$ corresponds to the probability of system failure, conditional to the value of the state vector $x_k \in \mathcal{R}^{n_{x_k}}$. Note that Eq (12) is a particular case of Eq. (13).

$$P(ToF \leq k) = \int_{\mathcal{R}^{n_{x_k}}} \mathcal{P}(failure \mid x_k) p(x_k \mid y_{1:k_p}) dx_k \tag{13}$$

Further, the authors in (Acuña and Orchard 2018, 2017) assert that this probability measure (Eq. (12)) has been misinterpreted as a Cumulative Mass Function (CMF) and is limited to cases of strictly degenerative systems. For the general case, (Acuña and Orchard 2018, 2017) propose that this concept should be reinterpreted as a Probability Mass Function (PMF) as the probability measure for ToF is defined at discrete time instants.

The authors in (Acuña and Orchard 2018, 2017) also state that a failure event can be treated as a non-stationary Bernoulli stochastic process in which probabilities vary as time evolves. They denote healthy and faulty systems (at the $k-th$ time instant) by $\mathcal{F}_k$ and $\mathcal{H}_k$, respectively, and characterize the true Probability of Failure (PoF) at the $k-th$ time instant, $P(\mathcal{F}_k)$ as:

$$P(\mathcal{F}_k) = \frac{P(\mathcal{F}_k, \mathcal{H}_{k_p:k-1})}{P(\mathcal{H}_{k_p:k-1} \mid \mathcal{F}_k)}, \quad \forall \quad k > k_p \tag{14}$$

Since $P(\mathcal{H}_{k_p:k-1} \mid \mathcal{F}_k)$ corresponds to the probability of staying healthy until time $k-1$, given that the failure occurred at time k, the authors note that $P(\mathcal{H}_{k_p:k-1} \mid \mathcal{F}_k) = 1$ (it is assumed that the system can only fail once).

Applying the definition of joint probability, Eq. (14) is then rewritten as:

$$P(\mathcal{F}_k) = P(\mathcal{F}_k | \mathcal{H}_{k_p:k-1}) P(\mathcal{H}_{k_p:k-1}), \quad \forall \quad k > k_p \tag{15}$$

where $P(\mathcal{F}_k | \mathcal{H}_{k_p:k-1})$ corresponds to the failure probability measure that has been used in (Orchard and Vachtsevanos 2009; Pola et al. 2015), equivalent to the expression in Eq. (13), i.e.,

$$\begin{aligned}P(\mathcal{F}_k | \mathcal{H}_{k_p:k-1}) &= \int_{\mathcal{R}^{n_x}} \mathcal{P}(failure \mid x_k) p(x_k \mid y_{1:k_p}) dx_k \\ &= \sum_{i=1}^{N} w^{(i)} \mathcal{P}(failure | X = x_k^{(i)})\end{aligned} \tag{16}$$

where the hazard zone is described by a mapping $h(x_k): \mathbb{R}^{n_x} \to [0,1]$,

$$h(x_k) := \mathcal{P}(failure \mid x_k) \tag{17}$$

and where $P(\mathcal{H}_{k_p:k-1})$ is the probability that the system is healthy until the $(k-1)-th$ time instant, that is,

$$\begin{aligned}P(\mathcal{H}_{k_p:k-1}) &= P(\mathcal{H}_{k-1} | \mathcal{H}_{k_p:k-2}) P(\mathcal{H}_{k_p:k-2}) \\ &= P(\mathcal{H}_{k-1} | \mathcal{H}_{k_p:k-2}) P(\mathcal{H}_{k-2} | \mathcal{H}_{k_p:k-3}) P(\mathcal{H}_{k_p:k-3}) \\ &\vdots \\ &= \prod_{j=k_p+1}^{k-1} P(\mathcal{H}_j | \mathcal{H}_{k_p:j-1})\end{aligned} \tag{18}$$

Then, as $P(\mathcal{H}_j | \mathcal{H}_{k_p:j-1}) = 1 - P(\mathcal{F}_j | \mathcal{H}_{k_p:j-1})$ and the failure is modeled through a Bernoulli stochastic process, it follows that:

$$P(\mathcal{H}_{k_p:k-1}) = \prod_{j=k_p+1}^{k-1} \left(1 - P(\mathcal{F}_j|\mathcal{H}_{k_p:j-1})\right) \quad (19)$$

Therefore, the failure probability described in Eq. (15) is defined as the product of $P(\mathcal{F}_k|\mathcal{H}_{k_p:k-1})$ and $P(\mathcal{H}_{k_p:k-1})$, where the first term corresponds to the likelihood of failure at $k-th$ time (assuming that the system was healthy for all previous moments). The second term indicates the probability that the system was actually healthy until the $(k-1)-th$ time instant.

To exemplify, suppose that until the instant $k_p+\tau-1$, the system was healthy for all previous moments so that $P(\mathcal{F}_{k_p+\tau-1}|\mathcal{H}_{k_p:k_p+\tau-2})=0$ and $P(\mathcal{H}_{k_p:k_p+\tau-2})=(1-0)=1$. Then suppose that at the instant $k_p+\tau$, realizations of the states reach a failure condition such that $P(\mathcal{F}_{k_p+\tau}|\mathcal{H}_{k_p:k_p+\tau-1})=0.1$. This latter value is used to compute the probability that the system is healthy until $k_p+\tau-1$, that is, $P(\mathcal{H}_{k_p:k_p+\tau-1})=(1-0)\cdot(1-0.1)=0.9$. At the next time step, $k_p+\tau+1$, suppose that realizations of the states reach a failure condition such that $P(\mathcal{F}_{k_p+\tau+1}|\mathcal{H}_{k_p:k_p+\tau})=0.15$ and $P(\mathcal{H}_{k_p:k_p+\tau})=(1-0)\cdot(1-0.1)\cdot(1-0.15)=0.765$.

In this regard, we would like to point out that Eq. (12), Eq. (13) and Eq. (16) do not incorporate information on the evolution of the fault indicators before the time instant k, that is, the trajectory of the fault indicator from k_p to $k-1$. As one can see, Eq. (16) (which is used later to evaluate Eq. (19)) is evaluated only for x_k. In other words, $\mathcal{P}(failure|x_k)$, that is, the *hazard zone,* is defined only for the $k-th$ time instant which leads to failure distributions that do not represent accurately the probability of failure up to and including time k. Proper failure distribution needs to be a trajectory-dependent probability instead of a state-dependent one.

For illustration purposes, consider a system that undergoes a failure when the fault indicator is below the value three (3), as described in Eq. (20):

$$P(failure|x_k) = \begin{cases} 1, & x_k \leq 3; \\ 0, & \text{otherwise.} \end{cases} \quad (20)$$

Consider also two trajectories of the fault indicator generated through Eq. (22) for ten (10) time steps as shown in Table 1. Then results of the computation of the failure distribution through Acuña's definition using Eq. (15) for these trajectories is shown in Table 2.

As can be seen from Table 2, the cumulative distribution function reaches the value one (1) at time step ten (10) even though one of the two trajectories never actually crossed the threshold. Also, note that the same results for $P(\mathcal{H}_{k_p:k-1})$ would have been obtained if variables were assumed to be independent, as in Eq. (21).

$$P(\mathcal{H}_{k_p:k-1}) = \prod_{i=k_p}^{k-1} P(H_i) \quad (21)$$

Table 1: Realizations of the fault indicator for 10 time steps.

k	1	2	3	4	5	6	7	8	9	10
Sample No.	x_k	x_k	x_k	x_k	x_k	x_k	x_k	x_k	x_k	x_k
1	3.55	3.30	3.34	3.45	3.23	3.22	3.18	3.44	3.43	3.23
2	3.26	3.09	2.89	2.82	3.00	2.81	2.56	2.65	2.47	2.05

Table 2: CDF and PMF of ToF through Acuña's definition, that is, Eq. (15), for realizations in Table 1.

k	1	2	3	4	5	6	7	8	9	10
$P(\mathcal{F}_k\|\mathcal{H}_{k_p:k-1})$	0.00	0.00	0.50	0.50	0.50	0.50	0.50	0.50	0.50	0.50
$P(\mathcal{H}_k)$	1.00	1.00	0.50	0.50	0.50	0.50	0.50	0.50	0.50	0.50
$P(\mathcal{H}_{k_p:k-1})$	1.00	1.00	1.00	0.50	0.25	0.13	0.06	0.03	0.02	0.01
$P(ToF=k)$	0.00	0.00	0.50	0.25	0.13	0.06	0.03	0.02	0.01	0.00
$P(ToF\leq k)$	**0.00**	**0.00**	**0.50**	**0.75**	**0.88**	**0.94**	**0.97**	**0.98**	**0.99**	**1.00**

5. COMPUTING FAILURE DISTRIBUTION WITH A WELL-DEFINED HAZARD ZONE AND AN ILL-DEFINED HAZARD ZONE

To further exemplify, consider the space state representation in Eq. (22) as the Markov process that describes a fault indicator that decreases over time,

$$x_k = \alpha \cdot x_{k-1} + w_{k-1} \quad \forall k \in \mathbb{N} \quad (22)$$

where $0<\alpha<1$ and w_k in this case denote an independent Gaussian random variable, that is, $w \sim N(0,\sigma)$.

Assuming that k_p is the time instant when predictions are made, and that the system undergoes failure when the fault indicator reaches a certain threshold value, the hazard zone is defined by Eq. (23),

$$h(\mathbf{x}) = \min(x_p, \ldots, x_{k-1}, x_k), \quad (23)$$

and the hazard zone indicator is defined by Eq. (24), which is equivalent to Eq. (7):

$$I(\mathbf{x}) = \begin{cases} 1, & h(\mathbf{x}) \leq threshold; \\ 0, & \text{otherwise.} \end{cases} \quad (24)$$

If comparison with zero is preferred, the hazard zone can be rewritten as in Eq. (25),

$$h(\mathbf{x}) = \min(x_p, \ldots, x_{k-1}, x_k) - threshold, \tag{25}$$

and the hazard zone indicator can be rewritten as in Eq. (26),

$$I(\mathbf{x}) = \begin{cases} 1, & h(\mathbf{x}) \leq 0; \\ 0, & \text{otherwise}. \end{cases} \tag{26}$$

For illustration purposes, ten (10) trajectories (with equal weighting) were generated through Eq. (22) for 10-steps forward with $\alpha = 0.97$ and $w \sim N(0, 0.3)$. Figure 1 and Table 3 shows a single realization for these trajectories. These trajectories can be interpreted as estimations of a decreasing health index *x* with a failure threshold of 3. Due to the nature of the Markov process the trajectories do not exhibit strictly monotonic behavior. While the average of the trajectories decreases (although there is no guarantee for that, either), individual trajectories migrate in and out of the failure region.

If the threshold value is set to 3, the evaluation of the hazard zone as defined in Eq. (25) for each trajectory is shown in Table 4 and the evaluation of the hazard zone indicator as defined in Eq. (26) is shown in Table 5.

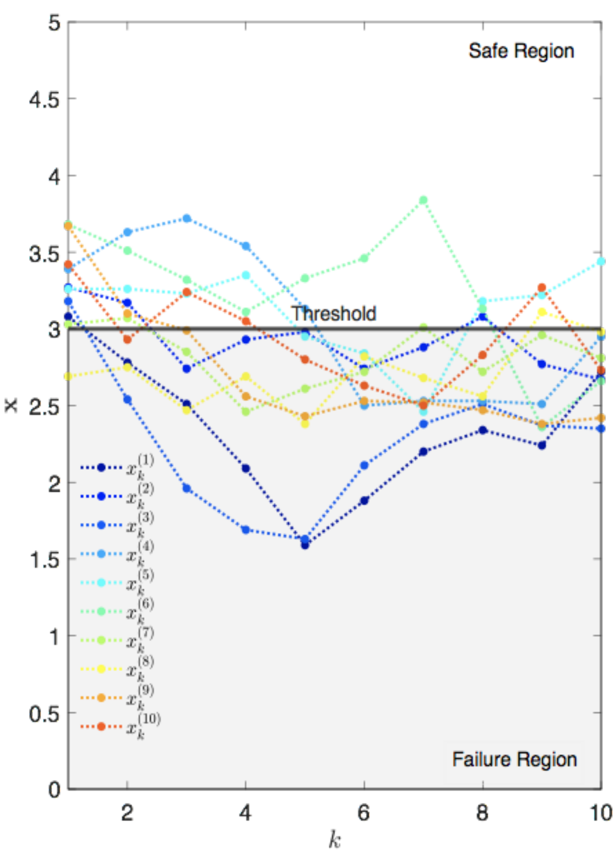

Figure 1: 10-steps trajectory prediction.

Table 3: Realizations of the fault indicator (Markov process in Eq. (22)) for 10 time steps.

k	1	2	3	4	5	6	7	8	9	10
Sample No.	x_k	x_k	x_k	x_k	x_k	x_k	x_k	x_k	x_k	x_k
1	3.08	2.78	2.51	2.09	1.59	1.88	2.20	2.34	2.24	2.72
2	3.27	3.17	2.74	2.93	2.98	2.74	2.88	3.08	2.77	2.67
3	3.18	2.54	1.96	1.69	1.63	2.11	2.38	2.51	2.37	2.35
4	3.39	3.63	3.72	3.54	3.13	2.50	2.53	2.53	2.51	2.95
5	3.26	3.26	3.23	3.35	2.95	2.84	2.46	3.18	3.22	3.44
6	3.68	3.51	3.32	3.11	3.33	3.46	3.84	3.13	2.36	2.66
7	3.03	3.07	2.85	2.46	2.61	2.72	3.01	2.72	2.96	2.81
8	2.69	2.75	2.47	2.69	2.38	2.82	2.68	2.56	3.11	2.98
9	3.67	3.10	2.99	2.56	2.43	2.53	2.52	2.47	2.38	2.42
10	3.42	2.93	3.24	3.05	2.80	2.63	2.50	2.83	3.27	2.73

Table 4: Evaluation of $h(\mathbf{x})$ (Eq. (25)) for realizations in Table 3.

k	1	2	3	4	5	6	7	8	9	10
Sample No.	$h(\mathbf{x})$	$h(\mathbf{x})$	$h(\mathbf{x})$	$h(\mathbf{x})$	$h(\mathbf{x})$	$h(\mathbf{x})$	$h(\mathbf{x})$	$h(\mathbf{x})$	$h(\mathbf{x})$	$h(\mathbf{x})$
1	0.1	-0.2	-0.5	-0.9	-1.4	-1.4	-1.4	-1.4	-1.4	-1.4
2	0.3	0.2	-0.3	-0.3	-0.3	-0.3	-0.3	-0.3	-0.3	-0.3
3	0.2	-0.5	-1.0	-1.3	-1.4	-1.4	-1.4	-1.4	-1.4	-1.4
4	0.4	0.4	0.4	0.4	0.1	-0.5	-0.5	-0.5	-0.5	-0.5
5	0.3	0.3	0.2	0.2	0.0	-0.2	-0.5	-0.5	-0.5	-0.5
6	0.7	0.5	0.3	0.1	0.1	0.1	0.1	0.1	-0.6	-0.6
7	0.0	0.0	-0.1	-0.5	-0.5	-0.5	-0.5	-0.5	-0.5	-0.5
8	-0.3	-0.3	-0.5	-0.5	-0.6	-0.6	-0.6	-0.6	-0.6	-0.6
9	0.7	0.1	0.0	-0.4	-0.6	-0.6	-0.6	-0.6	-0.6	-0.6
10	0.4	-0.1	-0.1	-0.1	-0.2	-0.4	-0.5	-0.5	-0.5	-0.5

Table 5: Evaluation of $I(\mathbf{x})$ (Eq. (26)) for realizations in Table 3.

k	1	2	3	4	5	6	7	8	9	10
Sample No.	$I(\mathbf{x})$	$I(\mathbf{x})$	$I(\mathbf{x})$	$I(\mathbf{x})$	$I(\mathbf{x})$	$I(\mathbf{x})$	$I(\mathbf{x})$	$I(\mathbf{x})$	$I(\mathbf{x})$	$I(\mathbf{x})$
1	0	**1**	**1**	**1**	**1**	**1**	**1**	**1**	**1**	**1**
2	0	0	**1**	**1**	**1**	**1**	**1**	**1**	**1**	**1**
3	0	**1**	**1**	**1**	**1**	**1**	**1**	**1**	**1**	**1**
4	0	0	0	0	0	**1**	**1**	**1**	**1**	**1**
5	0	0	0	0	**1**	**1**	**1**	**1**	**1**	**1**
6	0	0	0	0	0	0	0	0	**1**	**1**
7	0	0	**1**	**1**	**1**	**1**	**1**	**1**	**1**	**1**
8	**1**	**1**	**1**	**1**	**1**	**1**	**1**	**1**	**1**	**1**
9	0	0	**1**	**1**	**1**	**1**	**1**	**1**	**1**	**1**
10	0	**1**	**1**	**1**	**1**	**1**	**1**	**1**	**1**	**1**
$\sum_{i=1}^{10} I(\mathbf{x}^{(i)})$	**1**	**4**	**7**	**7**	**8**	**9**	**9**	**9**	**10**	**10**

Then, the computation of $P(ToF \leq k)$ for $k = 1$ is given by Eq. (10), that is:

$$\begin{aligned} \mathcal{P}(ToF \leq 1) &= \sum_{i=1}^{10} I(\mathbf{x}^{(i)}) \cdot 0.1 \\ &= \sum_{i=1}^{10} I(x_1^{(i)}) \cdot 0.1 \\ &= 1 \cdot 0.1 = 0.1 \end{aligned} \tag{27}$$

The computation of $P(ToF \leq k)$ for $k = 2$ is:

$$\begin{aligned} \mathcal{P}(ToF \leq 2) &= \sum_{i=1}^{10} I(\mathbf{x}^{(i)}) \cdot 0.1 \\ &= \sum_{i=1}^{10} I(x_1^{(i)}, x_2^{(i)}) \cdot 0.1 \\ &= 4 \cdot 0.1 = 0.4 \end{aligned} \tag{28}$$

and so on until $k = 10$:

$$\begin{aligned} \mathcal{P}(ToF \leq 10) &= \sum_{i=1}^{10} I(\mathbf{x}^{(i)}) \cdot 0.1^{(i)} \\ &= \sum_{i=1}^{10} I(x_1^{(i)}, \dots, x_9^{(i)}, x_{10}^{(i)}) \cdot 0.1^{(i)} \\ &= 10 \cdot 0.1 = 1 \end{aligned} \tag{29}$$

As a result, the CDF of ToF is shown in Fig. 2b.

On the other hand, consider again the space state representation in Eq. (22) as the Markov process that describes a fault indicator that decreases over time.

Assuming that the system undergoes a failure when the fault indicator reaches a certain threshold value, the hazard zone is now defined according to Eq. (17) as shown in Eq. (30),

$$h(x_k) = x_k - threshold \tag{30}$$

and the hazard zone indicator is defined by Eq. (31),

$$I(x_k) = \begin{cases} 1, & h(x_k) \leq 0; \\ 0, & \text{otherwise.} \end{cases} \tag{31}$$

The evaluation of the hazard zone as defined in Eq. (30) for each trajectory in Table 3 is shown in Table 6 and the evaluation of the hazard zone indicator as defined in Eq. (31) is shown in Table 7 .

Then, the computation of $P(ToF \leq k)$ for $k = 1$ is given by Eq. (10), that is:

Table 6: Evaluation of $h(x_k)$ (Eq. (30)) for realizations in Table 3.

k	1	2	3	4	5	6	7	8	9	10
Sample No.	$h(x_k)$	$h(x_k)$	$h(x_k)$	$h(x_k)$	$h(x_k)$	$h(x_k)$	$h(x_k)$	$h(x_k)$	$h(x_k)$	$h(x_k)$
1	0.1	-0.2	-0.5	-0.9	-1.4	-1.1	-0.8	-0.7	-0.8	-0.3
2	0.3	0.2	-0.3	-0.1	0.0	-0.3	-0.1	0.1	-0.2	-0.3
3	0.2	-0.5	-1.0	-1.3	-1.4	-0.9	-0.6	-0.5	-0.6	-0.6
4	0.4	0.6	0.7	0.5	0.1	-0.5	-0.5	-0.5	-0.5	-0.1
5	0.3	0.3	0.2	0.4	0.0	-0.2	-0.5	0.2	0.2	0.4
6	0.7	0.5	0.3	0.1	0.3	0.5	0.8	0.1	-0.6	-0.3
7	0.0	0.1	-0.1	-0.5	-0.4	-0.3	0.0	-0.3	0.0	-0.2
8	-0.3	-0.3	-0.5	-0.3	-0.6	-0.2	-0.3	-0.4	0.1	0.0
9	0.7	0.1	0.0	-0.4	-0.6	-0.5	-0.5	-0.5	-0.6	-0.6
10	0.4	-0.1	0.2	0.1	-0.2	-0.4	-0.5	-0.2	0.3	-0.3

Table 7: Evaluation of $I(x_k)$ (Eq. (31)) for realizations in Table 3.

k	1	2	3	4	5	6	7	8	9	10
Sample No.	$I(x_k)$	$I(x_k)$	$I(x_k)$	$I(x_k)$	$I(x_k)$	$I(x_k)$	$I(x_k)$	$I(x_k)$	$I(x_k)$	$I(x_k)$
1	0	**1**	**1**	**1**	**1**	**1**	**1**	**1**	**1**	**1**
2	0	0	**1**	**1**	**1**	**1**	**1**	0	**1**	**1**
3	0	**1**	**1**	**1**	**1**	**1**	**1**	**1**	**1**	**1**
4	0	0	0	0	0	**1**	**1**	**1**	**1**	**1**
5	0	0	0	0	**1**	**1**	**1**	0	0	0
6	0	0	0	0	0	0	0	0	**1**	**1**
7	0	0	**1**	**1**	**1**	**1**	0	**1**	**1**	**1**
8	**1**	**1**	**1**	**1**	**1**	**1**	**1**	**1**	0	**1**
9	0	0	**1**	**1**	**1**	**1**	**1**	**1**	**1**	**1**
10	0	**1**	0	0	**1**	**1**	**1**	**1**	0	**1**
$\sum_{i=1}^{10} I(x_k^{(i)})$	**1**	**4**	**6**	**6**	**8**	**9**	**8**	**7**	**7**	**9**

$$\begin{aligned} \mathcal{P}(ToF \leq 1) &= \sum_{i=1}^{10} I(x_1^{(i)}) \cdot 0.1 \\ &= 1 \cdot 0.1 = 0.1 \end{aligned} \tag{32}$$

The computation of $P(ToF \leq k)$ for $k = 2$ is:

$$\begin{aligned} \mathcal{P}(ToF \leq 2) &= \sum_{i=1}^{10} I(x_2^{(i)}) \cdot 0.1 \\ &= 4 \cdot 0.1 = 0.4 \end{aligned} \tag{33}$$

and so on until $k = 10$.

$$\mathcal{P}(ToF \leq 10) = \sum_{i=1}^{10} I(x_{10}^{(i)}) \cdot 0.1^{(i)} \\ = 9 \cdot 0.1 = 0.9 \quad (34)$$

As a result, the CDF of ToF is shown in Fig. 2c.

Note that the CDF in Fig. 2b (the CDF obtained for the first case where hazard zone is defined by Eq. (25) and hazard zone indicator is defined by Eq. (26)) is a ***monotonically increasing*** function that converges to value one when time tends to infinity, even when realizations of the fault indicator cross the threshold more than one time. In contrast, note that the CDF in Fig. 2c, (for CDF obtained for the second case when hazard zone is defined by Eq. (30) and the hazard zone indicator is defined by Eq. (31)) ***does not increase monotonically***. Although it may reach the value one, it does not necessarily converge to value one when time tends to infinity.

6. COMPUTING FAILURE DISTRIBUTION WITH THE CONVENTIONAL DEFINITION AND WITH ACUÑA'S DEFINITION.

The computation of the CDF of ToF is here repeated using the Acuña definition, that is, using Eq. (15), for dependent and independent variables. Results with Acuña's definition are then compared to the result obtained with Eq. (10).

Note that Eq. (15) corresponds to the failure probability at the time instant k, that is, $P(\mathcal{F}_k) = \mathcal{P}(ToF = k)$, while Eq. (10) correspond to the failure probability $\mathcal{P}(ToF \leq k)$. Therefore, computation of the CDF though Eq. (15) needs an additional step for the summation of the probabilities at previous time instants.

For the case of dependent variables, one hundred (100) trajectories (equal weighting) were generated through Eq. (22) for 10-steps forward with $\alpha = 0.97$ and $w \sim N(0, 0.2)$. Results for the computation of the CDF and PMF in this case are summarized in Table 8 and Table 9, and are shown in Fig. 3 and Fig. 5.

For the case of independent variables, one hundred (100) trajectories (equal weighting) were generated through Eq. (35) for 10-steps forward,

$$x_k = \mu_k + w_k \quad \forall k \in \mathbb{N}, \quad (35)$$

where $w \sim N(0, 0.2)$ and μ is a value in the interval $[2.3, 3.3]$ being $\mu_1 = \mathbf{3.3}$ and $\mu_{10} = \mathbf{2.3}$. Results for the computation of the CDF and PMF in this case are summarized in Table 10 and Table 11 and are shown in Fig. 4 and Fig. 6.

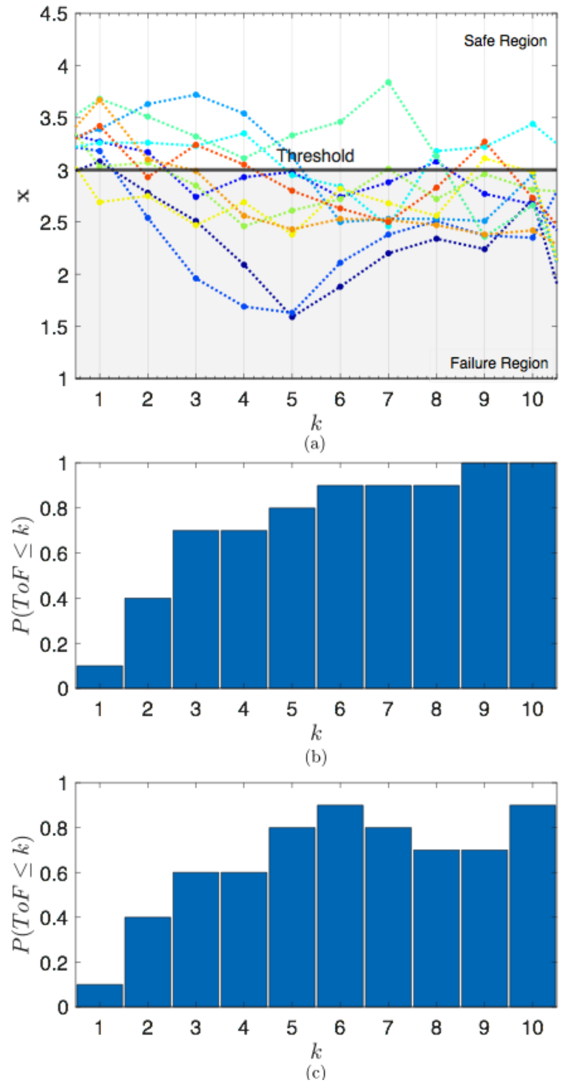

Figure 2: (a) 10-steps trajectory prediction. (b) CDF of ToF for realizations in Table 3 when the hazard zone is defined by Eq. (25) and the hazard zone indicator is defined by Eq. (26). (c) CDF of ToF for realizations in Table 3 when the hazard zone is defined by Eq. (30) and the hazard zone indicator is defined by Eq. (31).

Results obtained for dependent variables with Eq. (10) and with Acuña's definition differ, while results obtained for independent variables with Eq. (10) and with Acuña's definition are approximately the same. The latter results suggest that there is an underlying assumption of independence in the Acuña's definition. In particular, as mentioned earlier, the hazard zone in Acuña's definition (Eq. (17)) is defined as a function of the fault indicator at time k, without taking into account previous time instants. In other words, the hazard zone is defined in an independent manner. Consequently, Eq. (16) and Eq. (19) are also independent as discussed in Section 4.

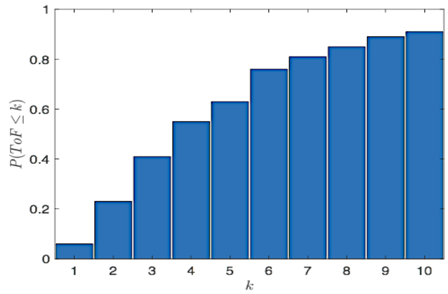

(a) Cumulative Density Function

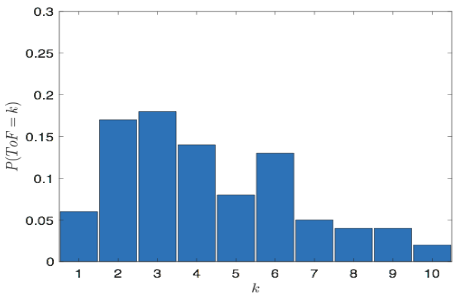

(b) Probability Mass Function

Figure 3: CDF and PMF of ToF through Eq. (10) for dependent variables.

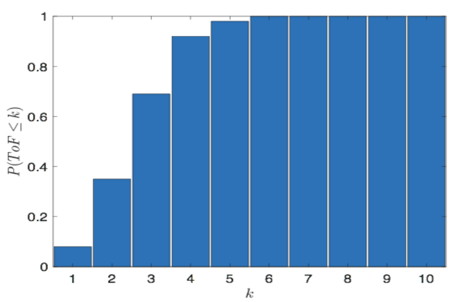

(a) Cumulative Density Function

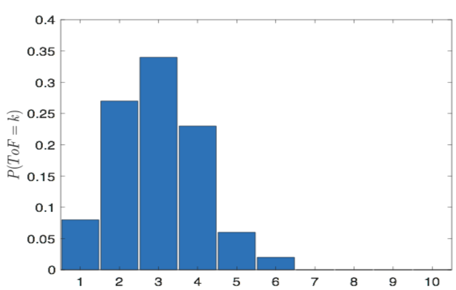

(b) Probability Mass Function

Figure 4: CDF and PMF of ToF through Eq. (10) for independent variables.

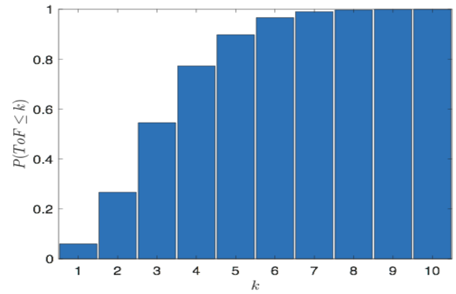

(a) Cumulative Density Function

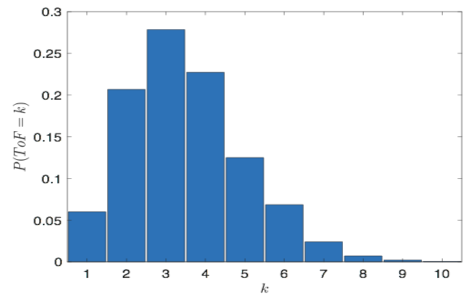

(b) Probability Mass Function

Figure 5: CDF and PMF of ToF through Acuña's definition, that is, Eq. (15), for dependent variables.

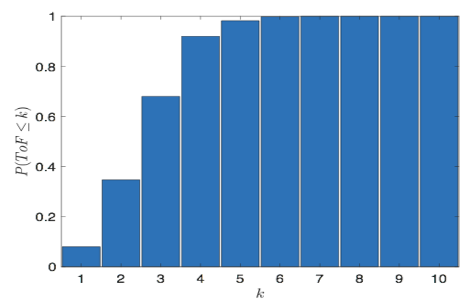

(a) Cumulative Density Function

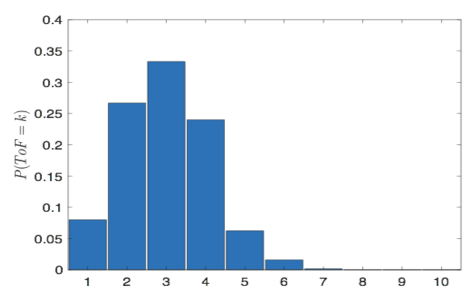

(b) Probability Mass Function

Figure 6: CDF and PMF of ToF through Acuña's definition, that is, Eq. (15), for independent variables.

Table 8: CDF and PMF of ToF through Eq. (10) for dependent variables.

k	1	2	3	4	5	6	7	8	9	10
$\mathcal{P}(ToF = k)$	**0.06**	**0.17**	**0.18**	**0.14**	**0.08**	**0.13**	**0.05**	**0.04**	**0.04**	**0.02**
$\mathcal{P}(ToF \leq k)$	**0.06**	**0.23**	**0.41**	**0.55**	**0.63**	**0.76**	**0.81**	**0.85**	**0.89**	**0.91**

Table 9: CDF and PMF of ToF through Acuña's definition, that is, Eq. (15), for dependent variables.

k	1	2	3	4	5	6	7	8	9	10
$P(\mathcal{F}_k \vert \mathcal{H}_{k_p:k-1})$	0.06	0.22	0.38	0.50	0.55	0.67	0.71	0.72	0.77	0.79
$P(\mathcal{H}_k)$	0.94	0.78	0.62	0.50	0.45	0.33	0.29	0.28	0.23	0.21
$P(\mathcal{H}_{k_p:k-1})$	1.00	0.94	0.73	0.45	0.23	0.10	0.03	0.01	0.00	0.00
$P(ToF = k)$	**0.06**	**0.21**	**0.28**	**0.23**	**0.13**	**0.07**	**0.02**	**0.01**	**0.00**	**0.00**
$P(ToF \leq k)$	**0.06**	**0.27**	**0.55**	**0.77**	**0.90**	**0.97**	**0.99**	**1.00**	**1.00**	**1.00**

Table 10: CDF and PMF of ToF through Eq. (10) for independent variables.

k	1	2	3	4	5	6	7	8	9	10
$\mathcal{P}(ToF = k)$	**0.08**	**0.27**	**0.34**	**0.23**	**0.06**	**0.02**	**0**	**0**	**0**	**0**
$\mathcal{P}(ToF \leq k)$	**0.08**	**0.35**	**0.69**	**0.92**	**0.98**	**1**	**1**	**1**	**1**	**1**

Table 11: CDF and PMF of ToF through Acuña's definition, that is, Eq. (15), for independent variables.

k	1	2	3	4	5	6	7	8	9	10
$P(\mathcal{F}_k \vert \mathcal{H}_{k_p:k-1})$	0.08	0.29	0.51	0.75	0.78	0.91	1.00	1.00	0.99	1.00
$P(\mathcal{H}_k)$	0.92	0.71	0.49	0.25	0.22	0.09	0.00	0.00	0.01	0.00
$P(\mathcal{H}_{k_p:k-1})$	1.00	0.92	0.65	0.32	0.08	0.02	0.00	0.00	0.00	0.00
$P(ToF = k)$	**0.08**	**0.27**	**0.33**	**0.24**	**0.06**	**0.02**	**0.00**	**0.00**	**0.00**	**0.00**
$P(ToF \leq k)$	**0.08**	**0.35**	**0.68**	**0.92**	**0.98**	**1.00**	**1.00**	**1.00**	**1.00**	**1.00**

Note also that cumulative distribution in Table 6 does not reach a value equal to 1 during the 10 time steps because not all trajectories crossed the threshold within those time steps. Nevertheless, cumulative distribution in Table 7 reaches a value equal to 1 despite of results in Table 7 correspond to the same trajectories in Table 6. Namely, despite that not all trajectories crossed the threshold.

7. CONCLUSION

Definitions in the literature on the computation of the CDF that describes the probability of failure up to and including time k, have suggested the use of state-dependent hazard zones instead of trajectory-dependent hazard zones. This may lead to a CDF that not always increases monotonically and that - although it may reach value one - does not necessarily converge to value one when time tends to infinity.

In this study we proposed an alternate definition of hazard zone which guarantees that: (*i*) the CDF is always an increasing function of time, even when realizations of the degradation process are not monotonic, (*ii*) the sum of all probabilities is always 1 and does not need to be normalized, and (*iii*) all probabilities are positive and less than or equal to 1. For illustration purposes, we computed the CDF for a simple degradation process using this alternative definition and using the definition previously reported in the literature.

We then compute the CDF using both the definition suggested here and using the Acuña's definition for dependent variables (the kind of variables encountered in the context of prognostic), and for independent variables. Results showed that both definitions provide approximately the same results only when variables are independent, which suggests an underlying assumption of independence in the Acuña's definition.

Our definition not only guarantees properties of the CDF but also provides a more straightforward definition for its computation in the context of prognostics. It should be noted that this work only considered the simplest hazard zone, namely a time-invariant and deterministic hazard zone. Future work will investigate time-variant and probabilistic hazard zones.

ACKNOWLEDGEMENT

This work was supported by the System-Wide Safety (SWS) project under the Airspace Operations and Safety Program within the NASA Aeronautics Research Mission Directorate (ARMD).

REFERENCES

Acuña, David E., and Marcos E. Orchard. 2017. "Particle-Filtering-Based Failure Prognosis via Sigma-Points: Application to Lithium-Ion Battery State-of-Charge Monitoring." *Mechanical Systems and Signal Processing*. https://doi.org/10.1016/j.ymssp.2016.08.029.

———. 2018. "A Theoretically Rigorous Approach to Failure Prognosis." In *Annual Conference Of The Prognostics And Health Management Society 2018*. Vol. 10. 1. Philadelphia,PA: PHM Society. https://doi.org/10.1234/phmconf.2018.v10i1.469.

Goebel, Kai, Matthew Daigle, Abhinav Saxena, and Indranil Roychoudhury. 2017. *Prognostics: The Science of Making Predictions*. CreateSpace Independent Publishing Platform.

Orchard, Marcos E., and George J. Vachtsevanos. 2009. "A Particle-Filtering Approach for on-Line Fault Diagnosis and Failure Prognosis." *Transactions of the Institute of Measurement and Control*. https://doi.org/10.1177/0142331208092026.

Pola, Daniel A., Hugo F. Navarrete, Marcos E. Orchard, Ricardo S. Rabie, Matias A. Cerda, Benjamin E. Olivares, Jorge F. Silva, Pablo A. Espinoza, and Aramis Perez. 2015. "Particle-Filtering-Based Discharge Time Prognosis for Lithium-Ion Batteries With a Statistical Characterization of Use Profiles." *IEEE Transactions on Reliability*. https://doi.org/10.1109/tr.2014.2385069.

Prob. Engineering Design. n.d. "Lecture Notes: Probabilistic Engineering Design." Missouri University of Science and

Technology. Accessed April 16, 2019. http://web.mst.edu/~dux/repository/me360/me360.html.

BIOGRAPHIES

Gina Sierra received the B.Sc. degree in Electronic Engineering (2008) and Master of Science in Information and Communications Technology (2013) from Universidad Distrital Francisco Jose de Caldas, Bogotá, Colombia, and Ph.D. degree in Electrical Engineering (2018) from the University of Chile. She has worked in the areas of Artificial Intelligence and Machine Learning with application in diverse domains and topics such as electric aircraft, telecommunications networks, and control systems. Since October 2018, she has been with SGT, Inc. at NASA Ames Research Center as a Research Engineer. Her current research interests include physics-based modeling and model-based diagnosis and prognosis.

Matthew Daigle is a Principal AI Scientist at NIO, Inc., where he works in the areas of artificial intelligence, machine learning, and data science for automotive applications, including vehicle health and autonomous driving. Prior to joining NIO, he was a Research Computer Scientist with NASA Ames Research Center from 2012 through 2017 and was the lead of the Diagnostics and Prognostics Group from 2016. From 2008 through 2011, he was an Associate Scientist with the University of California, Santa Cruz, at NASA Ames Research Center. He received the B.S. degree in computer science and computer and systems engineering from Rensselaer Polytechnic Institute, Troy, NY, in 2004, and the M.S. and Ph.D. degrees in computer science from Vanderbilt University, Nashville, TN, in 2006 and 2008, respectively. He has published over 100 peer-reviewed papers in the area of systems health management.

Kai Goebel is a Principal Scientist at Palo Alto Research Center where he investigates System Health for cyber physical systems. He is the founder and former director of the Prognostics Center of Excellence at NASA Ames Research Center (where much work reported in this article was conducted). After receiving the Ph.D. from the University of California at Berkeley in 1996, Dr. Goebel worked at General Electric's Corporate Research Center in Niskayuna, NY from 1997 to 2006 as a senior research scientist before joining NASA. He has carried out applied research in the areas of artificial intelligence, soft computing, and information fusion and his interest lies in advancing these techniques for real time monitoring, diagnostics, and prognostics. He holds 18 patents and has co-authored more than 350 publications in the area of systems health management.